Biosensors and Bioelectronics 102 (2018) 479–489

Contents lists available at ScienceDirect

Biosensors and Bioelectronics

journal homepage: www.elsevier.com/locate/bios

Nucleic acid-based electrochemical nanobiosensors

Alireza Abi[a], Zahra Mohammadpour[a], Xiaolei Zuo[b,*], Afsaneh Safavi[a,*]

[a] Department of Chemistry, Faculty of Sciences, Shiraz University, Shiraz 7194684795, Iran
[b] Division of Physical Biology & Bioimaging Center, Shanghai Synchrotron Radiation Facility, Shanghai Institute of Applied Physics, Chinese Academy of Sciences, Shanghai 201800, China

ARTICLE INFO

Keywords:
DNA
Aptamer
Nanomaterial
Electrochemical biosensor
Biomarker

ABSTRACT

The detection of biomarkers using sensitive and selective analytical devices is critically important for the early stage diagnosis and treatment of diseases. The synergy between the high specificity of nucleic acid recognition units and the great sensitivity of electrochemical signal transductions has already shown promise for the development of efficient biosensing platforms. Yet nucleic-acid based electrochemical biosensors often rely on target amplification strategies (e.g., polymerase chain reactions) to detect analytes at clinically relevant concentration ranges. The complexity and time-consuming nature of these amplification methods impede moving nucleic acid-based electrochemical biosensors from laboratory-based to point-of-care test settings. Fortunately, advancements in nanotechnology have provided growing evidence that the recruitment of nanoscaled materials and structures can enhance the biosensing performance (particularly in terms of sensitivity and response time) to the level suitable for use in point-of-care diagnostic tools. This Review highlights the significant progress in the field of nucleic acid-based electrochemical nanobiosensing with the focus on the works published during the last five years.

1. Introduction

Analytical devices enabling fast and cost-effective analysis of clinical samples are of growing demands for the early stage diagnosis and management of diseases. In this context, biosensors with electrochemical signal transductions hold great promise for the detection of trace levels of clinically relevant analytes. In comparison with mechanical- or optical-based sensing devices, electrochemical biosensors offer the advantages of low cost, simplicity, and the capability of being miniaturized. When integrated into lab-on-a-chip devices, electrochemical biosensors provide the possibility of analyzing small samples within short time frames, which is particularly useful for personalized therapy.

Centralized to any biosensing platform is biomolecular recognition. The development in biology over the past decades has proved that nucleic acids are not only hereditary materials for encoding genetic information but also ideal candidates for recognizing a variety of bioanalytes: deoxyribonucleic acid (DNA) and ribonucleic acid (RNA) can be easily detected through base-pairing with complementary nucleic acid probes, and non-nucleic acid targets can be specifically recognized by employing ligand-binding DNA or RNA sequences (aptamers). DNA tetrahedra, DNAzymes, and other functional DNA assemblies have further increased the attractiveness of nucleic acids for use in the design of electrochemical biosensors.

During the past 15 years, the field of nucleic acid-based electrochemical biosensing has witnessed great progress, thanks to the merging of biosensing research area with nanotechnology. Unprecedented biosensing opportunities have been achieved by employing nanomaterials with unique physicochemical properties in different aspects of electrochemical detection schemes. This has consequently propelled nanotechnology-based detection methods to the forefront of the biosensing research field. In the present Review, we highlight recent advances in the field of nucleic acid-based electrochemical nanobiosensors. We have itemized different classes of nanoscaled materials and structures that have been used in nucleic acid-based electrochemical biosensors and explained how they can contribute to the enhanced performance of such biosensors.

2. Nanoparticles

2.1. As electrode materials

Noble metal nanoparticles (NPs), with excellent conductivity, chemical inertness, and biocompatibility, have been extensively explored for improving the performance of nucleic acid-based electrochemical biosensors. As electrode modifiers, metal NPs can not only provide

* Corresponding authors.
E-mail addresses: zuoxiaolei@sinap.ac.cn (X. Zuo), safavi@susc.ac.ir, afsaneh_safavi@yahoo.com (A. Safavi).

https://doi.org/10.1016/j.bios.2017.11.019
Received 21 September 2017; Received in revised form 1 November 2017; Accepted 3 November 2017
Available online 04 November 2017
0956-5663/

large active surface area but also facilitate the electron transfer processes at the sensing interface, thereby imparting the biosensors high sensitivity (Xiang et al., 2017; Zhao et al., 2014). In the cases where metal NPs are employed as anchoring sites for probe molecules, the controlled immobilization and the suitable orientation of the capture probes on the electrode-supported NP islands may allow efficient biorecognition, which further improves the sensing sensitivity (de Oliveira Marques et al., 2009; Li et al., 2005). As a result of these unique properties, metal NPs-modified sensing interfaces have been fabricated and used for the electrochemical detection of a wide range of biologically relevant targets, including nucleic acids (M. Wang et al., 2014), proteins (Su et al., 2016a), cells (Chandra et al., 2013), amino acids (Liang et al., 2011), and pathogens (Chand and Neethirajan, 2017), among others. NPs of metal oxides such as IrO_2 (Mayorga-Martinez et al., 2015), TiO_2 (M. Wang et al., 2015), and ZrO_2 (Hu et al., 2011) have also been employed as electrode modifiers in nucleic acid-based electrochemical biosensors.

2.2. As redox tracers

Metal NPs can serve as tracers in electrochemical biosensors based on their redox properties. In the method developed by X. Li et al. (2015), a target DNA linked an Ag NP with a magnetic bead through base-pairing with partially complementary DNA strands attached to both particles. The formed sandwich complex was then injected into a cost-effective and user-friendly paper-based electrochemical device for DNA analysis. Based on the electrochemical signal of silver, they quantified a nucleotide sequence characteristic of DNA from hepatitis B virus (HBV) with a limit of detection (LOD) of 85 pM, which was not low enough for early detection of HBV. Measurements with higher sensitivity have been carried out by employing aggregates of NPs. As reported by Li et al. (2010), the use of Ag NP aggregate tags, which were ten times larger than the individual NPs, yielded a strong electrochemical signal that offered the possibility of detecting a HBV-related DNA at a concentration as low as 5 aM.

More recently, Song et al. (2014) realized multiplex protein analysis by employing two kinds of nucleic acid-modified Ag NP tags, each of which functionalized with aptamers specific to platelet-derived growth factor (PDGF-BB) and thrombin as well as DNA strands complementary to those on the other NP (Fig. 1). They used a disposable electrochemical array composing of four working electrodes of W1, W2, W3, and W4, which were functionalized with PDGF-BB-specific aptamers, thrombin-specific aptamers, a mixture of both, and irrelevant single-stranded DNAs (ssDNAs) as control, respectively. The presence of target mediated the formation of sandwich complexes between the relevant electrode-immobilized aptamers and the functionalized Ag NPs, which was followed by hybridization-induced formation of Ag NP aggregates. Sensitive analysis of the proteins was then performed by stripping voltammetric detection of the silver ions released from the Ag NP aggregates through a pre-oxidation step. Other than NP aggregates, the deposition of silver on Au NP tags (Zhu et al., 2013) or the use of NPs–loaded carriers (Zhu et al., 2012) was demonstrated to improve the detection sensitivity significantly. Also, biosensors based on the in situ DNA-templated syntheses of metal NPs and nanoclusters (NCs) have shown remarkable sensitivity toward nucleic acid and protein analysis (Y. Wang et al., 2017; Yang et al., 2015; Zhu et al., 2016).

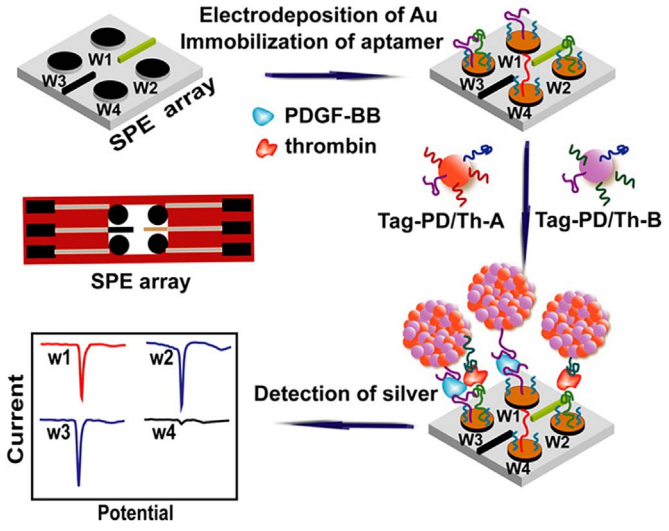

Fig. 1. Schematic representation of the electrochemical aptasensor for multiplex detection of PDGF-BB and thrombin. Reprinted with permission from Song et al. (2014). Copyright 2014 American Chemical Society.

2.3. As catalytic labels

Analogous to enzyme labels, some metal NPs can translate biorecognition events into significantly amplified signals by catalyzing a specific chemical reaction. The use of metal NP catalysts instead of enzymes in biosensing is beneficial as it allows overcoming the limitations associated with the poor thermal and environmental stability of enzymes. Moreover, in contrast to enzymes with only a small number of active sites (often just one), NP catalysts possess numerous active sites on their surface. As a result, when used as catalytic labels, NPs induce the generation of larger electrocatalytic signals than enzymes, thereby offering higher detection sensitivity. A typical detection scheme exploiting NPs catalytic properties for signal amplification relies on the target-mediated formation of a sandwich complex between a metal NP-linked reporter probe and an electrode-immobilized capture probe. The captured NP then causes the generation of a strong electrochemical signal by catalyzing the oxidation or reduction of a substrate, which can be used for the amplified detection of biomolecular targets (Hun et al., 2015; Polsky et al., 2006).

Other strategies relying on signal amplifications by NP-based catalytic labels have also been reported (Castañeda et al., 2017; de la Escosura-Muñiz et al., 2016; Li et al., 2012). Li et al. (2012) developed a reagentless method for hepatitis C virus (HCV) analysis by exploiting the hybridization-induced structural switching of a hairpin DNA probe immobilized on an electrode surface and conjugated to an Au NP at its free end. In the absence of the target DNA related to HCV genotype 1b, the stem-loop structure of the hairpin DNA kept the Au NP close to the electrode surface, allowing for efficient electron transfer with the electrode and enabling the electrocatalytic reduction of dissolved O_2. Upon hybridization, the stem-loop structure opened and the formed double-stranded DNA (dsDNA) moved the Au NP away from the electrode surface where the electron transfer was suppressed owing to the large distance. In a different methodology, de la Escosura-Muñiz et al. (2016) performed isothermal amplification of *Leishmania* DNA using primers labeled with magnetic beads and Au NPs. They magnetically collected the double-labeled DNA products on a screen-printed carbon electrode where the electrocatalytic activity of the Au NP tags toward the hydrogen evolution reaction allowed for detecting as low as 0.8 parasites per mL of blood (8×10^{-3} parasites per DNA amplification reaction).

In situ DNA-templated synthesis of metal NCs with electrocatalytic activities toward specific chemical reactions has recently been considered as an effective route for the amplified transduction of biorecognition events without the need for DNA functionalization of NCs. In this context, Z. Wang et al. (2015) developed a reusable microRNA (miRNA) sensor by taking advantage of the DNA/RNA heteroduplex-templated formation of Cu NCs and the electrocatalytic properties of these NCs toward hydrogen peroxide (H_2O_2) reduction. The sensor permitted sensitive quantification of target miRNAs with a LOD of 8.2 fM. In another study, Chen et al. (2015) combined target binding-triggered hybridization chain reactions (HCR) with the peroxidase-like activity of Ag NCs formed on cytosine-rich parts of the HCR-produced

long DNA duplexes to report a label-free signal-on aptasensor for lysozyme (detection limit 42 pM).

2.4. As carriers of signal elements

Because of the NPs high specific surface area, they can be loaded with a large number of signal elements and used for amplified detection of biomolecular targets. In sandwich-type detection strategies, the transduction of biorecognition events to electrochemical signals can be carried out through different routes, depending on the NPs functionalization. When NPs are solely functionalized with nucleic acid probes having no redox labels, the detection of targets is commonly achieved by electrochemical analysis of DNA binding electroactive molecules (e.g., $[Ru(NH_3)_6]^{3+}$) added to the solution (J. Xu et al., 2012). In contrast, NPs modified with redox-labeled DNA probes can generate electrochemical signals without the need for additional reagents (Z. Wang et al., 2014). The sensitivity of both detection schemes may, however, be compromised by binding of a single probe-functionalized NP to multiple DNA targets.

One way to surmount the limitation above is to introduce molecular spacers (e.g., DNA strands that are not complementary to targets) between the NP-immobilized reporter probes. The presence of the molecular spacers dilutes the reporter probe layer on the NP, thereby reducing the cross-reaction of the functionalized NP with multiple target biomolecules. The reduced cross-reaction can result in an enhanced sensitivity of the biosensor as more NPs can be brought to the electrode surface to form sandwich complexes. Z. Wang et al. (2014) demonstrated that the use of Au NPs modified with two kinds of redox-labeled DNA strands (of which one was complementary to the target DNA while the other was not) permitted the detection of DNA levels down to 50 fM. This LOD was much lower than the 1 pM detection limit obtained by Au NPs that were solely functionalized with the redox-labeled DNA strands complementary to the target DNA.

Besides sandwich-type detection strategies, other sensing approaches based on the use of NPs as signal element carriers have been reported (Jo et al., 2015; Lu et al., 2017; Tao et al., 2017; Wang et al., 2016). Jo et al. (2015) developed an aptasensor for cardiac troponin I (cTnI) detection down to 1.0 pM with the help of ferrocene (Fc)-modified silica NPs and the specific interaction between cTnI and its electrode-immobilized aptamers. When no target was present in the solution, the surface-confined aptamers allowed for the easy access of Fc-modified silica NPs to the electrode surface, resulting in a large Fc current response. In the presence of cTnI, however, the formation of cTnI/aptamer complex caused hindered access of the NPs to the electrode surface. More recently, Wang et al. (2016) exploited the hybridization-induced structural variation of electrode-immobilized hairpin DNA probes and the consequent change in the electrochemical signal of redox-tagged Au NPs attached to the free end of the hairpin probes for DNA sensing. In this reagentless approach, Au NPs were used as highly conductive platforms with large surface area for the immobilization of many redox-active melamine/Cu^{2+} complexes, which enabled sensitive analysis of DNA levels down to 1.2×10^{-19} M (ca. 15 DNA strands) by producing a large electrochemical signal.

NPs can also serve as supports to load enzymes or DNAzymes, which are able to provide amplified biorecognition signals by catalyzing a chemical reaction. By taking advantage of this feature of enzyme-loaded NPs, sensitive electrochemical detection of various bioanalytes, including nucleic acids (Wan et al., 2015), proteins (Zhou et al., 2013), cells (Chen et al., 2014a), and pathogens (Fu et al., 2014) has been reported. In a recent detection scheme developed by Wan et al. (2015), target DNA induced the formation of sandwich complexes between electrode-immobilized capture probes and reporter probe-linked Au NPs, which was followed by the deoxynucleotidyl transferase-catalyzed elongation of the reporter probes on the Au NPs (Fig. 2). During the DNA elongation, biotin moieties were incorporated into the generated long DNA strands and used for conjugating avidin-modified horseradish

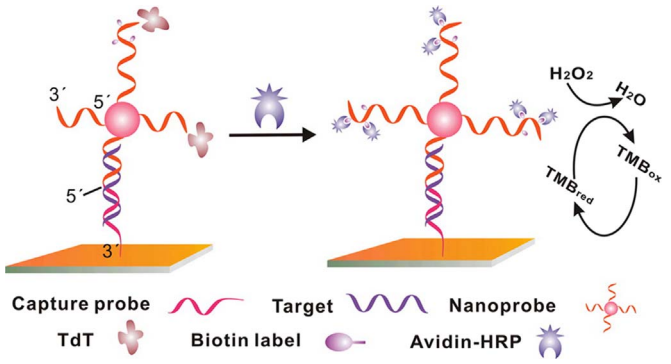

Fig. 2. Schematic representation of the electrochemical DNA biosensor that relies on the catalytic activity of multiple HRP molecules attached to Au NPs. Reprinted with permission from Wan et al. (2015). Copyright 2015 American Chemical Society.

peroxidase (HRP) molecules to the functionalized Au NPs. The numerous enzymes attached to the captured Au NPs then catalyzed the H_2O_2-mediated oxidation of 3,3′,5,5′−tetramethylbenzidine (TMB), thereby generating an amplified electrocatalytic signal. Using amperometry, analysis of the target DNA was carried out with a LOD of 10 fM.

2.5. As electron transfer regulators

The excellent conductivity of noble metal NPs has been explored for the development of biosensing methodologies in which the target binding can be detected through NPs-mediated electron transfer. Yang et al. (2014) developed an electrochemical DNA biosensor that relied on the noncovalent interaction of Au NPs with electrode-immobilized ssDNA probes and the resultant enhancement in the interfacial electron transfer process. As shown in Fig. 3, the ssDNA-bound Au NPs with large electroactive surface area served as conductive bridges to transfer electrons between the electrode and the negatively charged redox species ($[Fe(CN)_6]^{3-/4-}$) in the solution. Such Au NPs/DNA binding and the consequent enhancement in the electron transfer process were not observed after hybridization of the ssDNA probes with complementary target DNAs. Electrochemical impedance spectroscopy (EIS) permitted the detection of a breast cancer gene (BRCA1)-related DNA down to 1 pM without the need for NPs functionalization.

NPs can also be used as indicators of biorecognition reactions through inhibiting the interfacial electron transfer processes. In a thrombin aptasensing method reported by Deng et al. (2009), aptamer-functionalized Au NPs were brought on an electrode surface through the formation of sandwich complexes with electrode-immobilized secondary aptamers and thrombin molecules. Enlargement of the captured Au NPs via a gold deposition step followed by their coating with a negatively charged surfactant yielded large negatively charged NPs that

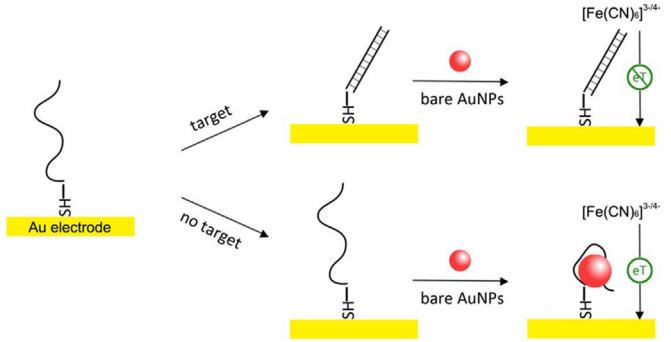

Fig. 3. Schematic illustration of the DNA sensing method based on Au NPs-mediated electron transfer between the electrode and $[Fe(CN)_6]^{3-/4-}$ redox species. Reprinted with permission from Yang et al. (2014). Copyright 2014 American Chemical Society.

impeded the electron transfer between the electrode and $[Fe(CN)_6]^{3-/4-}$ redox probes in the solution through two mechanisms: steric hindrance and electrostatic repulsion. Based on the variations in the interfacial electron transfer resistance recorded by EIS, thrombin was detectable at a low concentration of 100 fM.

2.6. As magnetic separators

The mobility of magnetic NPs (MNPs) in a reaction medium can be easily and effectively controlled by an external magnetic field. This property has intrigued scientists to employ MNPs in nucleic acid-based electrochemical biosensors for the separation, enrichment, or translocation of the biorecognition complexes. As an example, Fu et al. (2011) developed an electrochemical thrombin aptasensor in which the sandwich complexes formed from aptamer-functionalized Fe_3O_4 MNPs, thrombin molecules as the target, and secondary aptamer-wrapped single-walled carbon nanotubes (SWCNTs) were magnetically isolated and transferred onto a gold electrode surface. The addition of electroactive methylene blue (MB) to the solution followed by a magnetic removal step solely left carbon nanotubes (CNTs) with adsorbed MB molecules (MB can adsorb on CNTs through π– π stacking interactions) on the electrode surface. The CNTs-adsorbed MB produced a voltammetric signal corresponding to the thrombin concentration, which realized the detection of thrombin with a LOD of 3 pM. Methods for sensitive quantification of other bioanalytes using MNPs have also been reported in the literature (Feng et al., 2014; Kong et al., 2016; Mohamadi et al., 2015).

3. Nanosheets

3.1. As electrode materials

Thanks to the large surface area, high electrical conductivity, and wide electrochemical potential window of graphene, this two-dimensional (2D) nanomaterial has been widely employed as a sensitive platform for the detection of nucleic acids and other biomarkers (Ambrosi et al., 2014; Shuai et al., 2017). A classical approach for DNA sensing using graphene is to directly oxidize DNA bases on graphene-modified electrodes while recording the produced electrooxidation signal (Zhou et al., 2009). As the heterogeneous electron transfer kinetics at the edges of graphene nanosheets are significantly faster than that at their basal planes, the electrochemical activity of graphene-based electrodes was boosted by vertically aligning graphene sheets on a substrate (Akhavan et al., 2012) or increasing the density of edges via introducing artificial defects to graphene (Lim et al., 2010; Zribi et al., 2016). Also, graphene sheets doped with boron atoms, as p-type dopants (electron acceptors), exhibited enhanced sensitivity toward electrochemical oxidation of DNA bases (Tian et al., 2016).

The π-π stacking interactions between the aromatic rings of DNA bases and the hexagonal cells of graphene sheets have extensively been explored for diverse applications, particularly for bioanalysis (Tang et al., 2015). In the context of electrochemical DNA sensing, detection strategies commonly rely on the inferior interaction of electrode-supported graphene or its derivatives (e.g., thiofluorographene) with dsDNAs as compared to that with ssDNAs. In this sensing scheme, hybridization with targets causes DNA bases to be shielded inside the phosphate backbone of the formed double helices, resulting in a partial release of the DNA probes from the graphene sheets (Fig. 4). The target-induced unbinding of DNA probes from the graphene can then be electrochemically monitored, for example by EIS (Bonanni and Pumera, 2011; Urbanová et al., 2015). The noncovalent interaction of nucleic acids with graphene sheets has also been used for the detection of biomolecules other than nucleic acids (Ge et al., 2016; Wang et al., 2011).

While the π-π stacking interactions between graphene and nucleobases provide a facile route for biosensor fabrication, anchoring nucleic acid probes to graphene through covalent bonds may offer better sensing performance. Dubuisson et al. (2011) reported that covalent grafting of DNA probes onto anodized epitaxial graphene for DNA detection afforded a dynamic range that was three orders of magnitude wider than that obtained by DNA probe immobilization through π-π stacking interactions. The significantly wider dynamic range was attributed to the higher density of the covalently immobilized DNA probes. Consequently, covalent coupling of nucleic acid probes to graphene, which is typically realized through the amide bond formation between graphene carboxyl groups and amino-modified nucleic acids, has been extensively employed for the construction of efficint and robust electrochemical biosensors for bioanalytes ranging from nucleic acids (Seo et al., 2017) and proteins (Y. Wang et al., 2012) to cancer cells (Feng et al., 2011).

Recently, nanosheets of materials other than graphene have been used as platforms for the sensitive detection of biomarkers. X. Wang et al. (2015) prepared MoS_2 nanosheets via exfoliation of bulk MoS_2 and used them for label-free DNA sensing. The biosensor relied on the higher affinity of MoS_2 nanosheets for ssDNA probes than for DNA duplexes (formed upon target hybridization) and attained the detection of DNA at a concentration as low as 1.9×10^{-17} M. Yang et al. (2017) reported the use of ZnO nanosheets electrodeposited on thin layers of MoS_2 for the sensitive detection of DNA targets down to 6.6×10^{-16} M using MB as the hybridization indicator with different affinities for ssDNA and dsDNA. Also, Kumar et al. (2016) fabricated few-layer black phosphorus nanosheets and functionalized them with the positively charged poly-L-lysine, which facilitated the immobilization of myoglobin-specific aptamers via electrostatic interactions. Based on the redox activity of the heme groups in myoglobin, the biosensor afforded the detection of as low as 0.524 pg mL^{-1} myoglobin in serum samples.

3.2. As redox reporters

Redox active 2D nanomaterials such as graphene oxide (GO) nanoplatelets and MoS_2 nanoflakes can serve to translate biorecognition events into amplified electrochemical signals based on their direct redox activity (e.g., reduction of many oxygen-containing groups present on the surface of GO nanoplatelets). For this purpose, redox-active 2D nanomaterials are typically adsorbed on the electrode-immobilized DNA probes or target-specific aptamers through the π-π stacking interactions. The large redox signal of the nucleic acid-attached nanomaterials is then electrochemically recorded. In the presence of targets, however, a lower amount of the nanomaterials is adsorbed as a result of their weaker interaction with the formed DNA duplexes (Loo et al., 2014) or the partial removal of the target-bound aptamers from the electrode surface (Loo et al., 2013). Consequently, changes in the electrorochemical signals are observed in the presence of targets. This methodology has, for example, been applied for the analysis of DNA with a LOD of 500 pM (Bonanni et al., 2012) and thrombin within the concentration range from 3 pM to 0.3 μM (Loo et al., 2013).

3.3. As carriers of signal elements

The large specific surface area of graphene has made this nanomaterial suitable for carrying a large amount of signaling elements (e.g., redox indicators or enzymes), which can greatly amplify the biorecognition signal. In this context, several electrochemical aptasensors were fabricated based on the higher affinity of redox-loaded GO nanosheets for target-free aptamers than target-bound aptamers (Chen et al., 2013; T. Gao et al., 2015). In the absence of target, GO nanocarriers were attached to the electrode-tethered aptamers, and the signaling elements on the GO produced a large electrochemical signal. After aptamer-target binding, the GO nanocarriers were detached from the electrode surface, leading to a decrease in the redox signal.

In more desirable signal-on approaches, the biorecognition events bring graphene nanocarriers to the electrode surface, thereby

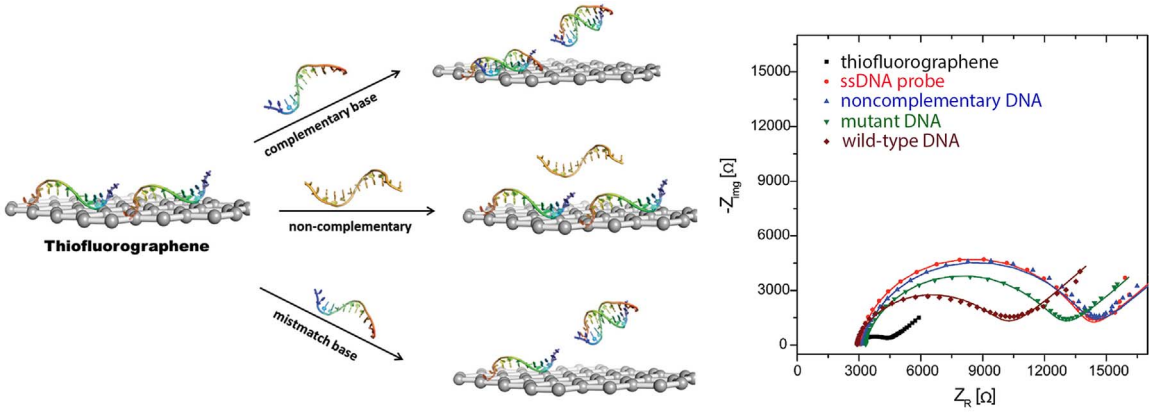

Fig. 4. Schematic illustration of the DNA sensing based on the hybridization-induced release of DNA probes from thiofluorographene, which can be measured by EIS. Adapted with permission from Urbanová et al. (2015). Copyright 2015 WILEY-VCH Verlag GmbH & Co. KGaA, Weinheim.

generating large electrochemical signals upon target binding. Q. Wang et al. (2013) employed electrode-tethered biotin-labeled hairpin DNA probes that upon hybridization made the biotin moieties accessible for binding to streptavidin- and ferric porphyrin (as a peroxidase mimic)-functionalized GO. Electroreduction of the species produced from the ferric porphyrin-mediated oxidation of *o*-phenylenediamine with H_2O_2 then yielded a large voltammetric current signal, which was used for the analysis of DNA (LOD of 22 aM). The use of graphene nanocarriers in sandwich-type detection strategies has also shown an increase in the detection signal upon target addition (Bai et al., 2012). More recently, a graphene nanocomposite coupled with three-way DNA junction-aided enzymatic target recycling strategy was used for the signal-on detection of lipopolysaccharide down to the femtogram level (Bai et al., 2014).

3.4. As electron transfer mediators

The excellent conductivity of graphene has recently been exploited to design biosensors and bioassays in which graphene mediates the electron transfer reactions involved in the signal transduction of biorecognition events. Feng et al. (2014) sandwiched an adenosine triphosphate (ATP) molecule between an aptamer-linked graphene and a secondary aptamer-functionalized MNP. The formed sandwich complex was magnetically transferred onto the surface of a self-assembled monolayer (SAM)-modified electrode, where graphene was released from the complex by the adenosine deaminase activity. The signal from graphene-mediated electron transfer between the electrode surface and redox species in the solution was recorded and used for the detection of ATP with a LOD of 13.6 nM.

Yan et al. (2013) exploited controlled assembly of graphene on an electrode surface for the development of a sensitive aptasensor for interferon-gamma (IFN-γ) analysis down to 0.065 pM. In their sensing scheme, the adsorption of IFN-γ-specific aptamers on graphene sheets prevented the assembly of the graphene on a SAM-modified electrode surface (Fig. 5). The presence of IFN-γ molecules led to the release of the aptamers from the graphene, which was followed by target recycling via DNase I-assisted cleavage of the desorbed aptamers. The obtained aptamer-free graphene was able to assemble on the SAM-modified electrode via hydrophobic interactions and effectively mediate the electron transfer between the electrode and electroactive redox species in the solution.

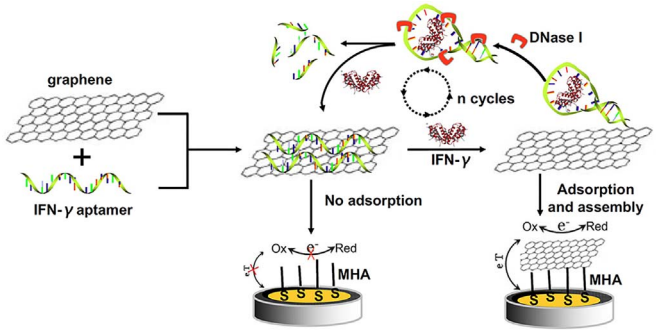

Fig. 5. Schematic representation of the methodology for IFN-γ detection based on graphene-mediated electron transfer between the electrode and electroactive redox species in the solution. Reprinted with permission from Yan et al. (2013). Copyright 2013 Elsevier.

4. Nanotubes and nanowires

4.1. As electrode materials

CNTs, with distinctive chemical, mechanical, and electronic properties, have been widely used as electrode materials in electrochemical biosensing (Tiwari et al., 2016). As an example, Yu et al. (2015) reported an electrochemical biosensor for the ratiometric determination of the human cellular prion protein (PrP^C) using a glassy carbon electrode (GCE) modified with multi-walled carbon nanotubes (MWCNTs)/β-cyclodextrin nanocomposite. The employment of MWCNTs improved the biosensor performance by increasing the conductivity and active surface area of the sensing platform, allowing for the sensitive and selective detection of PrP^C (LOD of 160 fM).

Through covalent attachment of nucleic acid probes to CNTs, bioanalytes such as nucleic acids (Tian et al., 2015) and proteins (Zelada-Guillén et al., 2013) have been detected. Covalent coupling of capture probes to CNTs can be achieved via the interaction between $–NH_2$ groups of amino-terminated oligonucleotides and activated carboxylic groups of CNTs or through the use of cross-linkers. As an example for the latter case, F. Li et al. (2015) employed polyamidoamine dendrimer for cross-linking carboxylated MWCNTs to carboxyl-terminated capture probes. They found that the dendrimer not only provided many amino groups for the immobilization of capture probes on MWCNTs but also decreased the undesired adsorption of the employed redox indicator (i.e., MB) on the MWCNTs surface. This methodology enabled sensitive analysis of miRNA-24 levels down to 0.5 fM.

It is known that ssDNA can wrap around SWCNTs through the π-π stacking interaction between nucleobases and aromatic sidewalls of CNTs. This unique interaction results in well-dispersed ssDNA/SWCNT hybrids with higher surface areas than aggregated CNTs, which is beneficial when an effective immobilization of molecules on these nanomaterials is of interest. Using a layer-by-layer electrostatic self-assembly approach, Kang et al. (2014) developed a high-throughput glucose biosensor by immobilizing negatively charged glucose oxidase on microelectrode-supported ssDNA/SWCNT hybrids through a thin

cationic polymer interlayer. Based on the direct electrochemistry of glucose oxidase on this microelectrode, they were able to detect glucose levels from 38 μM to 9.4 mM, which covers the glucose concentration range in normal human blood. Besides being used for molecular immobilization, ssDNA/SWCNT hybrids have been employed for the detection of target nucleic acids by electrochemical monitoring the dissociation of DNA probes from SWCNTs upon hybridizing with a complementary sequence (Li and Lee, 2015). Non-nucleic acid analytes have also been detected based on the target binding-induced release of aptamers from SWCNTs (Tang et al., 2012).

In comparison with randomly oriented nanotubes (NTs), vertically aligned NTs provide maximized access to the NTs surface, which can lead to an increase in the sensing sensitivity. Shi et al. (2015) reported on an ultrasensitive voltammetric detection of thrombin with a LOD of 3 fM using vertically aligned Au nanowires functionalized with thrombin-specific aptamers. The large surface area of the vertically aligned nanowire array provided numerous sites for the aptamer immobilization, and the proper distance between the adjacent nanowires facilitated the diffusion of the target analyte toward the nanowire-attached aptamers. In another study, Hu et al. (2015) reported on a biosensor for the in situ detection of unstable superoxide anion radical ($O_2^{\bullet -}$) secreted from the cells that were directly grown on a vertically aligned CNT array. This biosensing platform enabled the detection of unstable superoxide anion radicals (LOD of 30×10^{-9} M) shortly after they were released from the cells.

4.2. As carriers of signal elements

Owing to their high specific surface area, CNTs can load large amounts of signal elements (such as redox molecules or enzymes) on their sidewalls for amplified detection of bioanalytes. J. Li et al. (2015) exploited enzyme-loaded CNTs for the development of an ultrasensitive thrombin aptasensor. They modified MWCNTs with HRP and thrombin aptamers, which aided the formation of sandwich complexes between the functionalized MWCNTs, thrombin molecules, and GCE-immobilized secondary aptamers. MWCNTs-supported HRP then, in the presence of H_2O_2, catalyzed the oxidation of 3,3'-diaminobenzidine to form insoluble precipitates on the electrode surface. Electropolymerization of the insoluble precipitates on the electrode led to a substantial increase in the interfacial electron transfer resistance, which allowed for thrombin analysis with a detection limit of 0.05 pM. Taking advantage of the co-catalysis of hemin/G-quadruplex DNAzyme, platinum NPs, and flower-like MnO_2 nanospheres supported on MWCNTs, Xu et al. (2015) also succeeded at detecting thrombin concentration down to 0.040 pM.

Non-carbon one-dimensional nanostructures such as Au nanorods (Wen et al., 2016), Pt NTs (Sun et al., 2014), and Pt/Pd nanowires (Zhou et al., 2016) have also been fabricated and used as nanocarriers in nucleic-acid based biosensing. Sun et al. (2014) loaded porous Pt NTs with thrombin aptamers, glucose dehydrogenases, and hemin/G-quadruplex DNAzymes to sensitively quantify thrombin through a cascade of catalytic reactions (Fig. 6). In the presence of thrombin, the functionalized Pt NTs were captured on an electrode surface by forming sandwich complexes with secondary thrombin aptamers tethered to the electrode. A catalysis cascade was then initiated in the presence of glucose and β-nicotinamide adenine dinucleotide hydrate (NAD^+), yielding an amplified electrocatalytic signal. Using differential pulse voltammetry, a LOD of 0.15 pM was achieved.

4.3. As electron transfer mediators

The excellent electrical conductivity of CNTs has led scientists to employ these nanomaterials as electron transfer mediators in nucleic acid-based electrochemical biosensors. In a signal-on DNA sensing scheme developed by Nie et al. (2012), the presence of target DNA mediated the formation of sandwich complexes between ssDNA/CNT hybrids and hairpin DNA-functionalized magnetic beads. The formed sandwich complexes were then magnetically separated and transferred onto the surface of a SAM-modified gold electrode. Treatment with N,N-dimethylformamide caused the collected sandwiched complexes to release bare CNTs on the electrode surface. After magnetic beads removal, the bare CNTs mediated efficient electron transfer between the electrode and redox species in the solution, thus aiding the generation of an electrochemical signal proportional to the target concentration. The sensing method enabled the analysis of DNA fragments specific to HBV with a detection limit of 0.9 pM and single-base mismatch discrimination capability. Y. Wang et al. (2013) also employed CNTs as electron transfer mediators to detect methyltransferase activity.

5. DNA nanostructures

The evolution of DNA recognition elements from linear probes to tetrahedral nanostructures has provided a precise control over the orientation of surface-immobilized probes and the interprobe distance, which play important roles in the performance of biosensing platforms (Pei et al., 2013). Tetrahedral DNA nanostructures (TDNs) are typically formed from the self-assembly of four ssDNA sequences and can be immobilized on gold electrodes by the three vertices containing –SH functional groups. A pendant DNA strand at the top vertex, which projects outward, can be rationally designed to serve as a capture probe or as a binding site for the immobilization of a biorecognition element (e.g., an antibody).

The Fan group proposed several electrochemical sensing platforms for the sensitive analysis of target nucleic acids (Dong et al., 2015; Ge et al., 2014; Lin et al., 2014). They reported sandwich-based hybridization biosensors in which target DNA or miRNA strands mediate the formation of sandwich complexes between biotinylated reporter strands and DNA probes at the top vertex of the electrode-tethered TDNs. Avidin/HRP bioconjugates then bind to the formed sandwich complexes through the biotin-avidin interaction and catalyze the oxidation of a substrate (e.g., TMB) in the presence of H_2O_2. The redox activity of the product of the catalytic reaction at the electrode surface generates an electrocatalytic current, which can be used for the detection of target nucleic acids at the femtomolar level (Dong et al., 2015; Lin et al., 2014). Analysis down to 100 aM of DNA and 10 aM of miRNA was carried out by coupling TDNs-based sensing platforms with the HCR amplification method (Fig. 7), which involved the catalytic activity of multiple HRP molecules for every target binding event (Ge et al., 2014).

The potential of TDNs as scaffolds for protein analysis was explored through immobilizing target-specific aptamers or antibodies on the free vertex of the surface-bound TDNs (Chen et al., 2014b; Pei et al., 2010). Most notably, Chen et al. (2014b) reported that the use of TDNs offers controlled immobilization of the capture antibodies with a favorable orientation and intermolecular spacing. These characteristics effectively improved the binding efficiency and the detection sensitivity (LOD was determined as 0.5 ng/mL) of the biosensor for prostate-specific antigen (PSA) detection, as compared with the case when surface-confined dsDNAs were employed for antibody immobilization (LOD of 10 ng/mL). TDNs-based electrochemical platforms for the sensitive detection of other analytes such as *Escherichia coli* bacteria (Giovanni et al., 2015) and cancerous exosomes (S. Wang et al., 2017) have also been reported.

Besides TDNs, other DNA nanostructures have been exploited for the development of electrochemical biosensing platforms. Sheng et al. (2013) reported on the use of an electrode-tethered DNA nanostructure that was similar in shape to a triangular pyramid frustum for IFN-γ analysis. The presence of the target mediated restructuring of the electrode-immobilized DNA assembly from the "closed" to the "open" state, which caused a decrease in the interfacial electron transfer resistance. Using EIS, IFN-γ was detected with a low detection limit of 5.2×10^{-13} M. In another study, Zhang et al. (2015) implemented a DNA

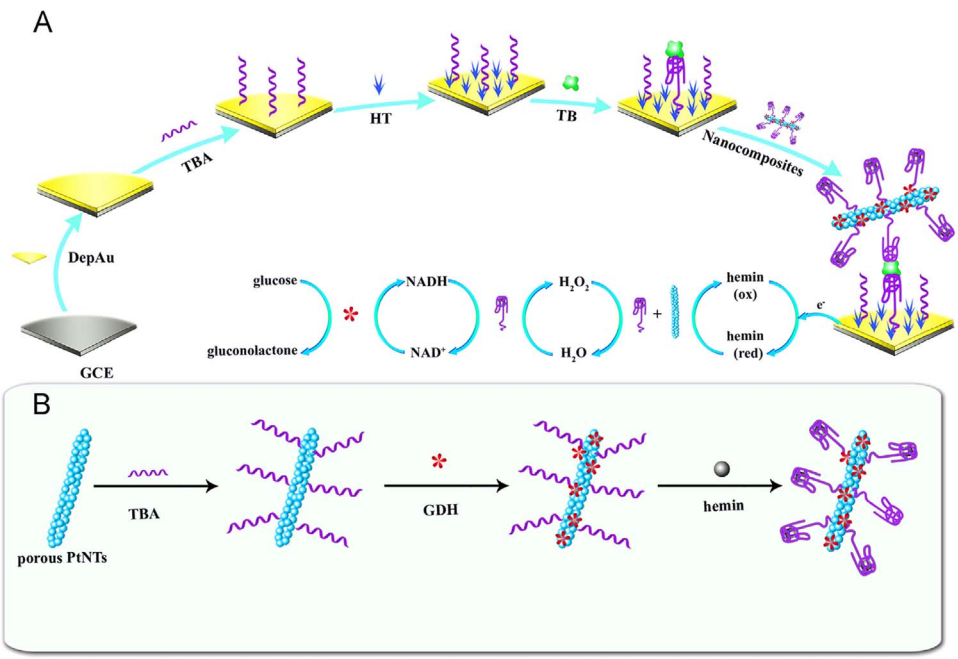

Fig. 6. (A) Schematic diagram of the thrombin aptasensor that takes advantage of the signal amplification through a catalysis cascade mediated by hemin/G-quadruplex DNAzyme- and glucose dehydrogenase (GDH)-loaded Pt NTs. (B) Schematic of the steps involved in the preparation of the functionalized Pt NTs. Reprinted with permission from Sun et al. (2014). Copyright 2014 Elsevier.

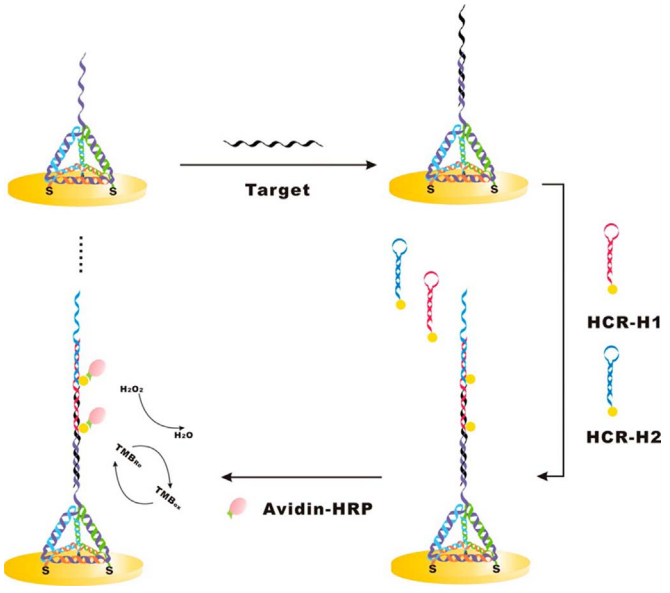

Fig. 7. Schematic illustration of the electrochemical biosensor for nucleic acid detection that takes advantage of the combined use of electrode-anchored TDNs and the HCR amplification method. Reprinted with permission from Ge et al. (2014). Copyright 2014 American Chemical Society.

three-way junction for DNA analysis based on the target-induced formation of electroactive hemin/G-quadruplexes on an electrode surface. Also, B. Liu et al. (2014) reported a homogeneous electrochemical sensing scheme based on the target-triggered structural rearrangement of an omega-like DNA nanostructure to an aptamer/DNAzyme conjugate. The formed DNAzyme then catalyzed the oxidation of *o*-phenylenediamine with the help of H_2O_2, producing an electrochemical signal that was used for the detection of ATP levels down to 0.6 pM. Target-triggered sequence extension of short electrode-tethered DNA strands into micrometer-long one-dimensional DNA nanostructures has also served as a strategy for the sensitive electrochemical analysis of nucleic acids (Chen et al., 2012).

In an immobilization-free sensing approach proposed by Xuan et al. (2015), target DNA strands induced the autonomous assembly of short DNAs and Fc-labeled peptide nucleic acids (PNAs) into dendritic DNA/PNA nanostructures through a cascade of toehold-mediated strand displacement reactions (Fig. 8). The incorporation of the uncharged Fc-labeled PNAs into the DNA/PNA nanostructures impeded the electron transfer between Fc molecules and a negatively charged electrode surface (owing to the electrostatic repulsion between the negatively charged nanostructures and the electrode). Therefore, the voltammetric current signal of Fc was less intense in a solution containing the target compared to the case of target-free solutions in which Fc-labeled PNAs would freely diffuse to the electrode surface. This methodology offered DNA detection down to 100 fM with excellent ability to differentiate between perfectly matched and single-nucleotide polymorphism (SNP)-containing sequences.

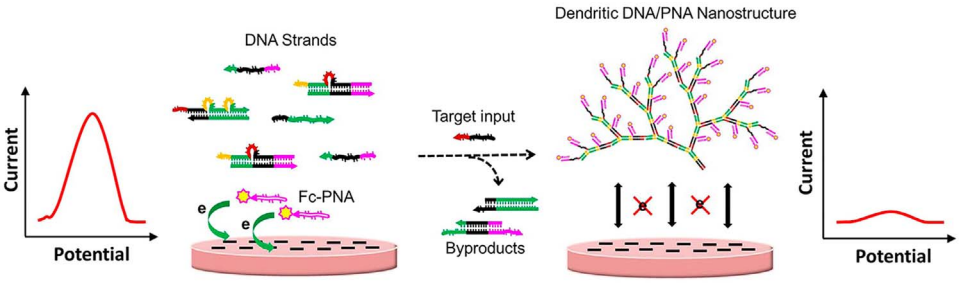

Fig. 8. Schematic illustration of the immobilization-free nucleic acid sensing strategy based on the target-induced self-assembly of dendritic DNA/PNA nanostructures. Adapted with permission from Xuan et al. (2015). Copyright 2015 American Chemical Society.

6. Nanoelectrodes

The term nanoelectrode typically refers to an electrode with at least one dimension below 100 nm. In comparison with conventional macroelectrodes, nanoelectrodes are characterized with small cell time constants and fast rate of mass transfers of redox species to and from the electrode surface. These features make nanoelectrodes suitable for rapid and sensitive electrochemical analysis. Most importantly, because of their small dimensions, nanoelectrodes have found applications in biological studies, for example for single-cell measurements (Cox and Zhang, 2012).

In the context of nucleic acid-based biosensing, researchers have designed both individual (Salamifar and Lai, 2014; Wang et al., 2018; Zhang et al., 2017) and arrays of nanoelectrodes (Silvestrini et al., 2013) with DNA or aptamer-functionalized surfaces. In a recent study, Peinetti et al. (2015) employed isolated Au NPs electrogenerated inside the cavities of a nanoporous alumina matrix as a nanoelectrode array for the label-free impedimetric detection of adenosine monophosphate (AMP). They functionalized the Au NPs with AMP-specific aptamers, and as the size of the nanoelectrodes was comparable with that of the aptamers, the small change in the aptamer structure upon AMP binding induced a substantial variation in the interfacial electron transfer properties. By measuring the changes in the electron transfer resistance upon target binding, they were able to analyze AMP in the nanomolar level. Au NPs electrodeposited on a GO surface, which showed the characteristic sigmoidal-shaped current-potential curves of nanoelectrodes, were also exploited as nanoelectrode arrays for bioanalysis (Z. Wang et al., 2012).

7. Nanochannels

Solid-state nanochannels and nanopores for controlled transportation of molecules and ions have been the subject of considerable research interest in the past years. In the field of electrochemical biosensing, nanoporous membranes with tunable pore size have been employed as sensing platforms for electrochemical detection of biomolecules (de la Escosura-Muñiz and Mekoçi, 2010). The sensing mechanism is typically based on the biorecognition reaction-induced steric or electrostatic effect (or both) inside the nanochannels of the membranes, which influences the diffusion flux of electroactive indicators passing through the channels. The alteration in the flux of the redox indicator is recorded by an electrode at one end of the membrane and used as the biorecognition signal. Remarkably, nanoporous membranes not only act as platforms for the detection of biomolecular targets but also serve as filters to minimize the interfering effects of micro-sized components present in complex biological matrices (de la Escosura-Muñiz et al., 2013).

H. L. Gao et al. (2015) covalently functionalized the nanochannels of a porous anodic alumina membrane with morpholino (a neutral analog of DNA). They then hybridized the immobilized morpholino strands with partially matched probe DNAs and utilized the probe DNA/morpholino-functionalized nanochannel array to identify SNPs in the PML/RARα fusion gene (a biomarker for acute promyelocytic leukemia). In this detection scheme, the fully matched or the SNP-containing DNA target competed with morpholino for the DNA probe to form target/probe DNA duplexes, which then flowed out of the nanochannels and left neutrally charged morpholino on the nanochannels inner walls (Fig. 9). This change in the nanochannels surface charge caused an alteration in the diffusion flux of the redox-active $[Fe(CN)_6]^{3-}$ molecules. Besides nucleic acids, non-nucleic acid targets such as thrombin (de la Escosura-Muñiz et al., 2013) and ATP (Yu et al., 2014) were also successfully detected by functionalizing the inner walls of nanochannel arrays with target-specific aptamers.

8. Nanostructured electrodes

Three-dimensional nanostructured electrodes with multidirectional nanoscaled features protruding from the surface provide large surface area for effective immobilization of nucleic acid probes. These electrodes have recently been exploited for the sensitive detection of a wide range of biomolecules, including nucleic acids and proteins, among others (J. Liu et al., 2014; Perumal et al., 2015; L. P. Xu et al., 2012). Notably, the sensitivity of such sensing platforms is critically dependent on the morphology of the nanostructured surfaces. Su et al. (2016b) reported that leaves-like gold dendrites synthesized on an indium tin oxide surface offered a lower detection limit (100 aM) for a target DNA than hierarchical flower-like or spherical gold nanostructures with 1 fM and 10 fM detection limits, respectively. The higher sensitivity of leaves-like gold dendrites was ascribed to the larger surface area and the higher degree of surface roughness of these nanostructures, aiding the accommodation of more probe DNAs with improved target capturing capabilities.

Similar to the research above, Soleymani et al. (2009b) showed that rough nanostructured microelectrodes (NMEs) display superior sensitivity toward DNA detection compared with smooth hemispherical microelectrodes. The enhanced sensitivity of NMEs was found to be primarily linked with the improved accessibility of surface-tethered probes for incoming target molecules, making biorecognition reactions faster and more efficient (Bin et al., 2010; Soleymani et al., 2009a). Indeed, the high deflection angle among DNA probes immobilized on high-curvature nanoscaled features of NMEs reduces the interaction between nearby DNA probes, thereby providing large interprobe spacing for target binding (Bin et al., 2010; De Luna et al., 2017). Furthermore, when coupled with the $[Ru(NH_3)_6]^{3+}/[Fe(CN)_6]^{3-}$ electrocatalytic reporter system, the favorable radial diffusion around the NMEs (as compared with the linear diffusion around smooth 2D platforms) leads to enhanced mass transports of redox species, generating enlarged electroanalytical signals (Safaei et al., 2016; Zhou et al., 2014). The development of such metallic NMEs for the sensitive detection of disease biomarkers, particularly small DNA and microRNA molecules at the femtomolar or attomolar concentration range, has been extensively investigated in Kelley's group (Besant et al., 2015; Das et al., 2012; Safaei et al., 2016; Sage et al., 2014).

Other than small-sized target nucleic acids, the challenge for the rapid and sensitive detection of slow-moving large nucleic acid molecules (e.g., messenger RNAs or mRNAs) was addressed by increasing the size of NMEs from 5 to 100 μm while maintaining the high level of surface nanostructuring (Soleymani et al., 2011). The three-dimensional branches of these NMEs effectively shorten the hybridization time by being accessible to a large portion of sample volumes, facilitating the collision of slow-moving targets with the probe-functionalized NMEs. Using these relatively large NMEs, highly sensitive detection of, for example, bcr-abl gene fusion specific to chronic myeloid leukemia (Vasilyeva et al., 2011) or PSA mRNA (Ivanov et al., 2013) was accomplished within short time frames ($\leq$ 1 h). Bacterial pathogens related to infectious diseases were also successfully analyzed based on the detection of their specific mRNA on NMEs (Das and Kelley, 2013; Lam et al., 2013). Furthermore, NMEs have been integrated into sample-to-answer devices for bacterial detection (Lam et al., 2012) or mRNA profiling of circulating tumor cells (CTCs) isolated from whole blood (Mohamadi et al., 2015). In the work reported by Mohamadi et al. (2015), CTCs were magnetically captured inside a fluidic device using antibody-functionalized MNPs (Fig. 10). Following an in situ electrochemical cell lysis step, the lysate was transfered to a chamber housing a set of PNA probe-functionalized NMEs ($\sim$ 20 μm in diameter), which allowed for highly sensitive detection of PSA mRNAs released from as few as 2 cancer cells per mL of blood samples within 1 h.

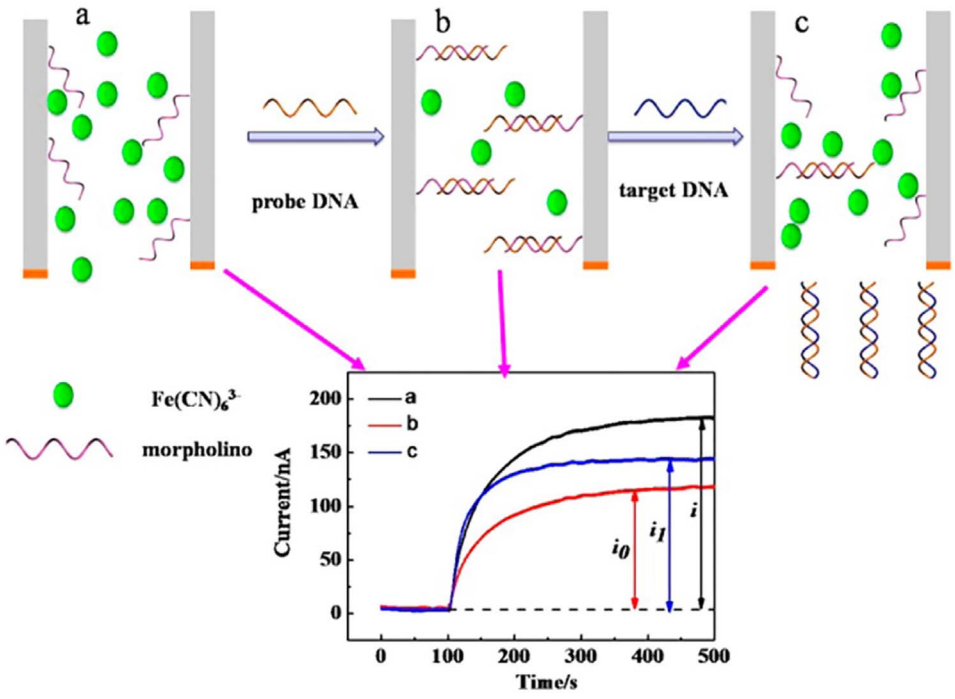

Fig. 9. Schematic representation of the DNA sensing device that relies on the biorecognition-induced changes in the transportation of redox indicators through the nanochannel. Reprinted with permission from H. L. Gao et al. (2015). Copyright 2015 American Chemical Society.

9. Conclusion and outlook

The emergence of nanotechnology has opened novel horizons for developing new generations of nucleic acid-based electrochemical biosensors. In this review article, we highlighted some of the most recent advancements in the field of nucleic acid-based electrochemical nanobiosensing that have been made by employing nanomaterials and nanostructured electrodes in the design of the biosensors. In some cases, nanomaterials provided high conductivity and enlarged surface areas for efficient probe immobilization or acted as reporter units for amplified transduction of biorecognition events. In some others, the favored orientation of biomolecular probes on nanostructured materials and interfaces resulted in efficient target recognition. The enhanced mass transfer of redox molecules toward nanostructured electrodes, the effective isolation of biorecognition complexes by MNPs, and the novel sensing opportunities offered by nanochannels and nanoelectrodes are among other interesting features that originate from combining nanotechnology and biosensing research fields. The overall outcome of the

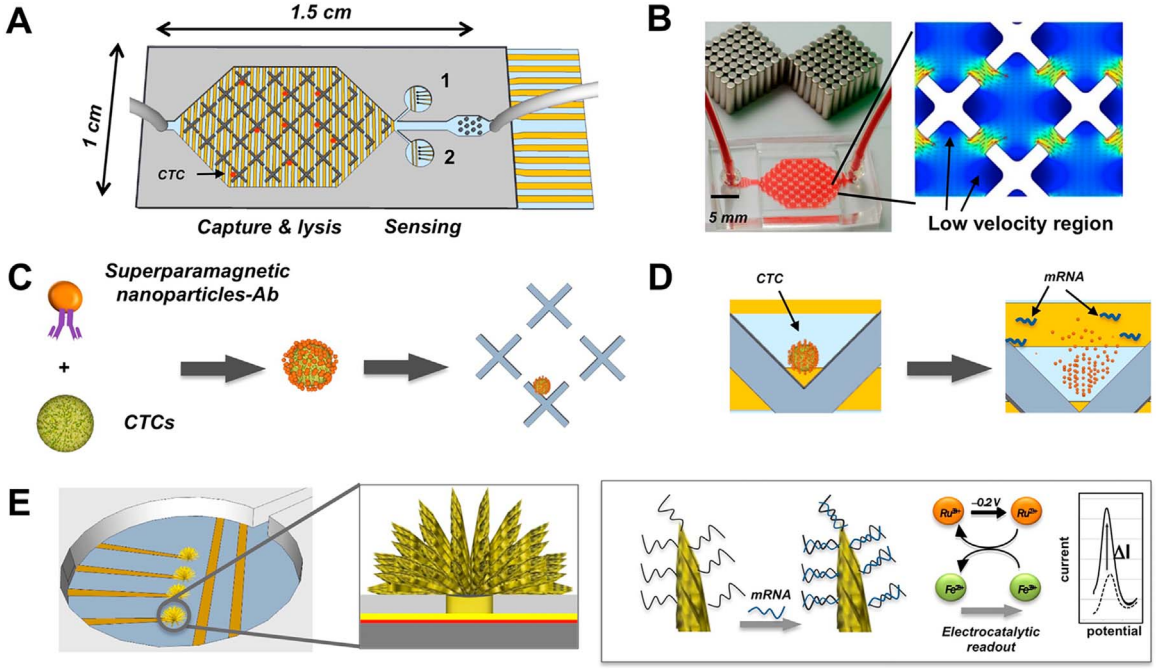

Fig. 10. The design of the sample-to-answer device for the capture and mRNA profiling of CTCs. (A) Schematic of the integrated chip featuring capture structures, electrochemical lysis electrodes, and NME sensors; (B) photographs of the fluidic capture device (left) and the flow velocity profile within the capture chamber (right); (C) selective labeling of target CTCs with antibody-functionalized MNPs and magnetically capturing the labeled cells in the vicinity of the trapping structures; (D) electrochemical lysis of the captured cells by lysis electrodes; (E) electrochemical analysis of mRNA released from the captured CTCs on the surface of PNA probe-functionalized NMEs using the $[Ru(NH_3)_6]^{3+}/[Fe(CN)_6]^{3-}$ electrocatalytic reporter system. Reprinted with permission from Mohamadi et al. (2015). Copyright 2015 American Chemical Society.

implementation of nanomaterials and nanostructured interfaces appeared in the improved performance of the developed nanobiosensors, particularly in terms of the sensitivity and response time.

In spite of the low detection limit and short response time of the nanobiosensors that have hitherto been developed, some issues are still needed to be addressed before these analytical tools can be commercialized for real-world applications. In this context, the instability of some materials used in the nanobiosensing methods is one of the main concerns. For example, the tendency of nanomaterials, such as nanoparticles, to aggregate can adversely affect the reliability of the obtained test results. The relatively poor stability of natural nucleic acids can also limit the practical applications of nucleic acid-based biosensors. Overcoming the hurdles mentioned above may be achieved through the development and use of highly stable nanomaterials and artificial nucleic acids with superior stability to their natural counterparts.

The non-specific adsorption caused by the complex matrix of biological samples (e.g., whole blood) is another major issue that faces electrochemical nanobiosensors on their way to clinical analysis. It is, therefore, critically important to design the sensing interfaces resistant to non-specific adsorption. Alternatively, nanobiosensors can be integrated into lab-on-a-chip devices wherein sample matrices are simplified by a separation unit before being directed toward the detection electrodes. Such bioanalytical tools will also raise the capability of multiplex analysis of different analytes (e.g., DNAs, RNAs, proteins, cells, small biomolecules, and pathogens), which can revolutionize disease diagnosis and therapeutics toward personalized medicine. Advances in microfluidic fabrication technologies is expected to provide cost-effective device architectures that can be integrated with nanobiosensors and thereby put nucleic acid-based electrochemical nanobiosensors squarely on the road to clinics.

Acknowledgments

We wish to acknowledge the Iran's National Elites Foundation, Shiraz University Research Council, and Chinese Academy of Sciences for the support of this work.

Conflicts of interest

There are no conflicts to declare.

References

Akhavan, O., Ghaderi, E., Rahighi, R., 2012. ACS Nano 6, 2904–2916.
Ambrosi, A., Chua, C.K., Bonanni, A., Pumera, M., 2014. Chem. Rev. 114, 7150–7188.
Bai, L., Chai, Y., Pu, X., Yuan, R., 2014. Nanoscale 6, 2902–2908.
Bai, L., Yuan, R., Chai, Y., Yuan, Y., Wang, Y., Xie, S., 2012. Chem. Commun. 48, 10972–10974.
Besant, J.D., Das, J., Burgess, I.B., Liu, W., Sargent, E.H., Kelley, S.O., 2015. Nat. Commun. 6, 6978.
Bin, X., Sargent, E.H., Kelley, S.O., 2010. Anal. Chem. 82, 5928–5931.
Bonanni, A., Chua, C.K., Zhao, G., Sofer, Z., Pumera, M., 2012. ACS Nano 6, 8546–8551.
Bonanni, A., Pumera, M., 2011. ACS Nano 5, 2356–2361.
Castañeda, A.D., Brenes, N.J., Kondajji, A., Crooks, R.M., 2017. J. Am. Chem. Soc. 139, 7657–7664.
Chand, R., Neethirajan, S., 2017. Biosens. Bioelectron. 98, 47–53.
Chandra, P., Noh, H.B., Shim, Y.B., 2013. Chem. Commun. 49, 1900–1902.
Chen, J.R., Jiao, X.X., Luo, H.Q., Li, N.B., 2013. J. Mater. Chem. B 1, 861–864.
Chen, L., Sha, L., Qiu, Y.W., Wang, G.F., Jiang, H., Zhang, X., 2015. Nanoscale 7, 3300–3308.
Chen, X., Hong, C.Y., Lin, Y.H., Chen, J.H., Chen, G.N., Yang, H.H., 2012. Anal. Chem. 84, 8277–8283.
Chen, X., Wang, Y., Zhang, Y., Chen, Z., Liu, Y., Li, Z., Li, J., 2014a. Anal. Chem. 86, 4278–4286.
Chen, X., Zhou, G., Song, P., Wang, J., Gao, J., Lu, J., Fan, C., Zuo, X., 2014b. Anal. Chem. 86, 7337–7342.
Cox, J.T., Zhang, B., 2012. Annu. Rev. Anal. Chem. 5, 253–272.
Das, J., Cederquist, K.B., Zaragoza, A.A., Lee, P.E., Sargent, E.H., Kelley, S.O., 2012. Nat. Chem. 4, 642–648.
Das, J., Kelley, S.O., 2013. Anal. Chem. 85, 7333–7338.
de la Escosura-Muñiz, A., Baptista-Pires, L., Serrano, L., Altet, L., Francino, O., Sánchez, A., Merkoçi, A., 2016. Small 12, 205–213.
de la Escosura-Muñiz, A., Chunglok, W., Surareungchai, W., Merkoçi, A., 2013. Biosens. Bioelectron. 40, 24–31.
de la Escosura-Muñiz, A., Mekoçi, A., 2010. Chem. Commun. 46, 9007–9009.
De Luna, P., Mahshid, S.S., Das, J., Luan, B., Sargent, E.H., Kelley, S.O., Zhou, R., 2017. Nano Lett. 17, 1289–1295.
de Oliveira Marques, P.R.B., Lermo, A., Campoy, S., Yamanaka, H., Barbé, J., Alegret, S., Pividori, M.I., 2009. Anal. Chem. 81, 1332–1339.
Deng, C., Chen, J., Nie, Z., Wang, M., Chu, X., Chen, X., Xiao, X., Lei, C., Yao, S., 2009. Anal. Chem. 81, 739–745.
Dong, S., Zhao, R., Fan, C., Hao, R., Song, H., 2015. ACS Appl. Mater. Interfaces 7, 8834–8842.
Dubuisson, E., Yang, Z., Loh, K.P., 2011. Anal. Chem. 83, 2452–2460.
Feng, L., Chen, Y., Ren, J., Qu, X., 2011. Biomaterials 32, 2930–2937.
Feng, L., Zhang, Z., Ren, J., Qu, X., 2014. Biosens. Bioelectron. 62, 52–58.
Fu, Y., Callaway, Z., Lum, J., Wang, R., Lin, J., Li, Y., 2014. Anal. Chem. 86, 1965–1971.
Fu, Y., Wang, T., Bu, L., Xie, Q., Li, P., Chen, J., Yao, S., 2011. Chem. Commun. 47, 2637–2639.
Gao, H.L., Wang, M., Wu, Z.Q., Wang, C., Wang, K., Xia, X.H., 2015. Anal. Chem. 87, 3936–3941.
Gao, T., Liu, F., Yang, D., Yu, Y., Wang, Z., Li, G., 2015. Anal. Chem. 87, 5683–5689.
Ge, L., Wang, W., Sun, X., Hou, T., Li, F., 2016. Anal. Chem. 88, 2212–2219.
Ge, Z., Lin, M., Wang, P., Pei, H., Yan, J., Shi, J., Huang, Q., He, D., Fan, C., Zuo, X., 2014. Anal. Chem. 86, 2124–2130.
Giovanni, M., Setyawati, M.I., Tay, C.Y., Qian, H., Kuan, W.S., Leong, D.T., 2015. Adv. Funct. Mater. 25, 3840–3846.
Hu, F.X., Kang, Y.J., Du, F., Zhu, L., Xue, Y.H., Chen, T., Dai, L.M., Li, C.M., 2015. Adv. Funct. Mater. 25, 5924–5932.
Hu, R., Wu, Z.S., Zhang, S., Shen, G.L., Yu, R., 2011. Chem. Commun. 47, 1294–1296.
Hun, X., Xie, G., Luo, X., 2015. Chem. Commun. 51, 7100–7103.
Ivanov, I., Stojcic, J., Stanimirovic, A., Sargent, E., Nam, R.K., Kelley, S.O., 2013. Anal. Chem. 85, 398–403.
Jo, H., Gu, H., Jeon, W., Youn, H., Her, J., Kim, S.K., Lee, J., Shin, J.H., Ban, C., 2015. Anal. Chem. 87, 9869–9875.
Kang, Z., Yan, X., Zhang, Y., Pan, J., Shi, J., Zhang, X., Liu, Y., Choi, J.H., Porterfield, D.M., 2014. ACS Appl. Mater. Interfaces 6, 3784–3789.
Kong, D., Bi, S., Wang, Z., Xia, J., Zhang, F., 2016. Anal. Chem. 88, 10667–10674.
Kumar, V., Brent, J.R., Shorie, M., Kaur, H., Chadha, G., Thomas, A.G., Lewis, E.A., Rooney, A.P., Nguyen, L., Zhong, X.L., Burke, M.G., Haigh, S.J., Walton, A., McNaughter, P.D., Tedstone, A.A., Savjani, N., Muryn, C.A., O'Brien, P., Ganguli, A.K., Lewis, D.J., Sabherwal, P., 2016. ACS Appl. Mater. Interfaces 8, 22860–22868.
Lam, B., Das, J., Holmes, R.D., Live, L., Sage, A., Sargent, E.H., Kelley, S.O., 2013. Nat. Commun. 4, 2001.
Lam, B., Fang, Z., Sargent, E.H., Kelley, S.O., 2012. Anal. Chem. 84, 21–25.
Li, C.Z., Liu, Y., Luong, J.H.T., 2005. Anal. Chem. 77, 478–485.
Li, F., Peng, J., Zheng, Q., Guo, X., Tang, H., Yao, S., 2015. Anal. Chem. 87, 4806–4813.
Li, H., Sun, Z., Zhong, W., Hao, N., Xu, D., Chen, H.Y., 2010. Anal. Chem. 82, 5477–5483.
Li, J., Lee, E.C., 2015. Biosens. Bioelectron. 71, 414–419.
Li, J., Wang, J., Guo, X., Zheng, Q., Peng, J., Tang, H., Yao, S., 2015. Anal. Chem. 87, 7610–7617.
Li, W., Wu, P., Zhang, H., Cai, C., 2012. Chem. Commun. 48, 7877–7879.
Li, X., Scida, K., Crooks, R.M., 2015. Anal. Chem. 87, 9009–9015.
Liang, J., Chen, Z., Guo, L., Li, L., 2011. Chem. Commun. 47, 5476–5478.
Lim, C.X., Hoh, H.Y., Ang, P.K., Loh, K.P., 2010. Anal. Chem. 82, 7387–7393.
Lin, M., Wen, Y., Li, L., Pei, H., Liu, G., Song, H., Zuo, X., Fan, C., Huang, Q., 2014. Anal. Chem. 86, 2285–2288.
Liu, B., Zhang, B., Chen, G., Tang, D., 2014. Chem. Commun. 50, 1900–1902.
Liu, J., Wagan, S., Dávila Morris, M., Taylor, J., White, R.J., 2014. Anal. Chem. 86, 11417–11424.
Loo, A.H., Bonanni, A., Ambrosi, A., Pumera, M., 2014. Nanoscale 6, 11971–11975.
Loo, A.H., Bonanni, A., Pumera, M., 2013. Nanoscale 5, 4758–4762.
Lu, J.Y., Zhang, X.X., Huang, W.T., Zhu, Q.Y., Ding, X.Z., Xia, L.Q., Luo, H.Q., Li, N.B., 2017. Anal. Chem. 89, 9734–9741.
Mayorga-Martinez, C.C., Chamorro-Garcia, A., Serrano, L., Rivas, L., Quesada-Gonzalez, D., Altet, L., Francino, O., Sanchez, A., Merkoci, A., 2015. J. Mater. Chem. B 3, 5166–5171.
Mohamadi, R.M., Ivanov, I., Stojcic, J., Nam, R.K., Sargent, E.H., Kelley, S.O., 2015. Anal. Chem. 87, 6258–6264.
Nie, H., Yang, Z., Huang, S., Wu, Z., Wang, H., Yu, R., Jiang, J., 2012. Small 8, 1407–1414.
Pei, H., Lu, N., Wen, Y., Song, S., Liu, Y., Yan, H., Fan, C., 2010. Adv. Mater. 22, 4754–4758.
Pei, H., Zuo, X., Pan, D., Shi, J., Huang, Q., Fan, C., 2013. NPG Asia Mater. 5, e51.
Peinetti, A.S., Ceretti, H., Mizrahi, M., González, G.A., Ramírez, S.A., Requejo, F.G., Montserrat, J.M., Battaglini, F., 2015. Nanoscale 7, 7763–7769.
Perumal, V., Hashim, U., Gopinath, S.C.B., Haarindraprasad, R., Foo, K.L., Balakrishnan, S.R., Poopalan, P., 2015. Sci. Rep. 5, 12231.
Polsky, R., Gill, R., Kaganovsky, L., Willner, I., 2006. Anal. Chem. 78, 2268–2271.
Safaei, T.S., Das, J., Mahshid, S.S., Aldridge, P.M., Sargent, E.H., Kelley, S.O., 2016. Adv. Healthcare Mater. 5, 893–899.
Sage, A.T., Besant, J.D., Lam, B., Sargent, E.H., Kelley, S.O., 2014. Acc. Chem. Res. 47, 2417–2425.
Salamifar, S.E., Lai, R.Y., 2014. Anal. Chem. 86, 2849–2852.
Seo, D.H., Pineda, S., Fang, J., Gozukara, Y., Yick, S., Bendavid, A., Lam, S.K.H., Murdock, A.T., Murphy, A.B., Han, Z.J., Ostrikov, K.K., 2017. Nat. Commun. 8, 14217.
Sheng, Q.L., Liu, R.X., Zheng, J.B., Zhu, J.J., 2013. Nanoscale 5, 7505–7511.

Shi, L., Chu, Z., Liu, Y., Jin, W., 2015. J. Mater. Chem. B 3, 3134–3140.
Shuai, H.L., Wu, X., Huang, K.J., 2017. J. Mater. Chem. B 5, 5362–5372.
Silvestrini, M., Fruk, L., Ugo, P., 2013. Biosens. Bioelectron. 40, 265–270.
Soleymani, L., Fang, Z., Lam, B., Bin, X., Vasilyeva, E., Ross, A.J., Sargent, E.H., Kelley, S.O., 2011. ACS Nano 5, 3360–3366.
Soleymani, L., Fang, Z., Sargent, E.H., Kelley, S.O., 2009a. Nat. Nanotechnol. 4, 844–848.
Soleymani, L., Fang, Z., Sun, X., Yang, H., Taft, B.J., Sargent, E.H., Kelley, S.O., 2009b. Angew. Chem. Int. Ed. 48, 8457–8460.
Song, W., Li, H., Liang, H., Qiang, W., Xu, D., 2014. Anal. Chem. 86, 2775–2783.
Su, S., Sun, H., Cao, W., Chao, J., Peng, H., Zuo, X., Yuwen, L., Fan, C., Wang, L., 2016a. ACS Appl. Mater. Interfaces 8, 6826–6833.
Su, S., Wu, Y., Zhu, D., Chao, J., Liu, X., Wan, Y., Su, Y., Zuo, X., Fan, C., Wang, L., 2016b. Small 12, 3794–3801.
Sun, A., Qi, Q., Wang, X., Bie, P., 2014. Biosens. Bioelectron. 57, 16–21.
Tang, J., Tang, D., Zhou, J., Yang, H., Chen, G., 2012. Chem. Commun. 48, 2627–2629.
Tang, L., Wang, Y., Li, J., 2015. Chem. Soc. Rev. 44, 6954–6980.
Tao, Y., Yin, D., Jin, M., Fang, J., Dai, T., Li, Y., Li, Y., Pu, Q., Xie, G., 2017. Biosens. Bioelectron. 96, 99–105.
Tian, H., Wang, L., Sofer, Z., Pumera, M., Bonanni, A., 2016. Sci. Rep. 6, 33046.
Tian, Q., Wang, Y., Deng, R., Lin, L., Liu, Y., Li, J., 2015. Nanoscale 7, 987–993.
Tiwari, J.N., Vij, V., Kemp, K.C., Kim, K.S., 2016. ACS Nano 10, 46–80.
Urbanová, V., Holá, K., Bourlinos, A.B., Čépe, K., Ambrosi, A., Loo, A.H., Pumera, M., Karlický, F., Otyepka, M., Zbořil, R., 2015. Adv. Mater. 27, 2305–2310.
Vasilyeva, E., Lam, B., Fang, Z., Minden, M.D., Sargent, E.H., Kelley, S.O., 2011. Angew. Chem. Int. Ed. 50, 4137–4141.
Wan, Y., Wang, P., Su, Y., Wang, L., Pan, D., Aldalbahi, A., Yang, S., Zuo, X., 2015. ACS Appl. Mater. Interfaces 7, 25618–25623.
Wang, D., Xiao, X., Xu, S., Liu, Y., Li, Y., 2018. Biosens. Bioelectron. 99, 431–437.
Wang, L., Zhu, C., Han, L., Jin, L., Zhou, M., Dong, S., 2011. Chem. Commun. 47, 7794–7796.
Wang, M., Fu, Z., Li, B., Zhou, Y., Yin, H., Ai, S., 2014. Anal. Chem. 86, 5606–5610.
Wang, M., Zhai, S., Ye, Z., He, L., Peng, D., Feng, X., Yang, Y., Fang, S., Zhang, H., Zhang, Z., 2015. Dalton Trans. 44, 6473–6479.
Wang, Q., Gao, F., Ni, J., Liao, X., Zhang, X., Lin, Z., 2016. Sci. Rep. 6, 22441.
Wang, Q., Lei, J., Deng, S., Zhang, L., Ju, H., 2013. Chem. Commun. 49, 916–918.
Wang, S., Zhang, L., Wan, S., Cansiz, S., Cui, C., Liu, Y., Cai, R., Hong, C., Teng, I.T., Shi, M., Wu, Y., Dong, Y., Tan, W., 2017. ACS Nano 11, 3943–3949.
Wang, X., Nan, F., Zhao, J., Yang, T., Ge, T., Jiao, K., 2015. Biosens. Bioelectron. 64, 386–391.
Wang, Y., He, X., Wang, K., Su, J., Chen, Z., Yan, G., Du, Y., 2013. Biosens. Bioelectron. 41, 238–243.
Wang, Y., Xiao, Y., Ma, X., Li, N., Yang, X., 2012. Chem. Commun. 48, 738–740.
Wang, Y., Zhang, X., Zhao, L., Bao, T., Wen, W., Zhang, X., Wang, S., 2017. Biosens. Bioelectron. 98, 386–391.
Wang, Z., Si, L., Bao, J., Dai, Z., 2015. Chem. Commun. 51, 6305–6307.
Wang, Z., Zhang, J., Yin, Z., Wu, S., Mandler, D., Zhang, H., 2012. Nanoscale 4, 2728–2733.
Wang, Z., Zhang, J., Zhu, C., Wu, S., Mandler, D., Marks, R.S., Zhang, H., 2014. Nanoscale 6, 3110–3115.
Wen, W., Huang, J.Y., Bao, T., Zhou, J., Xia, H.X., Zhang, X.H., Wang, S.F., Zhao, Y.D., 2016. Biosens. Bioelectron. 83, 142–148.
Xiang, J., Pi, X., Chen, X., Xiang, L., Yang, M., Ren, H., Shen, X., Qi, N., Deng, C., 2017. Biosens. Bioelectron. 96, 268–274.
Xu, J., Jiang, B., Su, J., Xiang, Y., Yuan, R., Chai, Y., 2012. Chem. Commun. 48, 3309–3311.
Xu, L.P., Wang, S., Dong, H., Liu, G., Wen, Y., Wang, S., Zhang, X., 2012. Nanoscale 4, 3786–3790.
Xu, W., Xue, S., Yi, H., Jing, P., Chai, Y., Yuan, R., 2015. Chem. Commun. 51, 1472–1474.
Xuan, F., Fan, T.W., Hsing, I.M., 2015. ACS Nano 9, 5027–5033.
Yan, G., Wang, Y., He, X., Wang, K., Liu, J., Du, Y., 2013. Biosens. Bioelectron. 44, 57–63.
Yang, C., Shi, K., Dou, B., Xiang, Y., Chai, Y., Yuan, R., 2015. ACS Appl. Mater. Interfaces 7, 1188–1193.
Yang, T., Chen, M., Kong, Q., Luo, X., Jiao, K., 2017. Biosens. Bioelectron. 89, 538–544.
Yang, Y., Li, C., Yin, L., Liu, M., Wang, Z., Shu, Y., Li, G., 2014. ACS Appl. Mater. Interfaces 6, 7579–7584.
Yu, J., Zhang, L., Xu, X., Liu, S., 2014. Anal. Chem. 86, 10741–10748.
Yu, P., Zhang, X., Zhou, J., Xiong, E., Li, X., Chen, J., 2015. Sci. Rep. 5, 16015.
Zelada-Guillén, G.A., Tweed-Kent, A., Niemann, M., Göringer, H.U., Riu, J., Rius, F.X., 2013. Biosens. Bioelectron. 41, 366–371.
Zhang, L., Guo, S., Zhu, J., Zhou, Z., Li, T., Li, J., Dong, S., Wang, E., 2015. Anal. Chem. 87, 11295–11300.
Zhang, Y., Xu, S., Xiao, X., Liu, Y., Qian, Y., Li, Y., 2017. Chem. Commun. 53, 2850–2853.
Zhao, J., Hu, S., Zhong, W., Wu, J., Shen, Z., Chen, Z., Li, G., 2014. ACS Appl. Mater. Interfaces 6, 7070–7075.
Zhou, J., Lai, W., Zhuang, J., Tang, J., Tang, D., 2013. ACS Appl. Mater. Interfaces 5, 2773–2781.
Zhou, M., Zhai, Y., Dong, S., 2009. Anal. Chem. 81, 5603–5613.
Zhou, X., Xue, S., Jing, P., Xu, W., 2016. Biosens. Bioelectron. 86, 656–663.
Zhou, Y.G., Wan, Y., Sage, A.T., Poudineh, M., Kelley, S.O., 2014. Langmuir 30, 14322–14328.
Zhu, Y., Chandra, P., Shim, Y.B., 2013. Anal. Chem. 85, 1058–1064.
Zhu, Y., Wang, H., Wang, L., Zhu, J., Jiang, W., 2016. ACS Appl. Mater. Interfaces 8, 2573–2581.
Zhu, Z., Gao, F., Lei, J., Dong, H., Ju, H., 2012. Chem. Eur. J. 18, 13871–13876.
Zribi, B., Castro-Arias, J.M., Decanini, D., Gogneau, N., Dragoe, D., Cattoni, A., Ouerghi, A., Korri-Youssoufi, H., Haghiri-Gosnet, A.-M., 2016. Nanoscale 8, 15479–15485.